Cancer Cell
Article

# *ETV6-NTRK3* Fusion Oncogene Initiates Breast Cancer from Committed Mammary Progenitors via Activation of AP1 Complex

Zhe Li,[1,4,5] Cristina E. Tognon,[6,9] Frank J. Godinho,[1,3,9] Laura Yasaitis,[1] Hanno Hock,[1,4,5,10] Jason I. Herschkowitz,[7] Chris L. Lannon,[6] Eunah Cho,[8] Seong-Jin Kim,[8,11] Roderick T. Bronson,[4] Charles M. Perou,[7] Poul H. Sorensen,[6] and Stuart H. Orkin[1,2,3,4,5,*]

[1]Division of Hematology/Oncology, Children's Hospital Boston
[2]Department of Pediatric Oncology, Dana Farber Cancer Institute
[3]Howard Hughes Medical Institute
[4]Harvard Medical School
[5]Harvard Stem Cell Institute
Boston, MA 02115, USA
[6]Department of Molecular Oncology, British Columbia Cancer Research Centre, Vancouver, British Columbia V5Z 1L3, Canada
[7]Departments of Genetics and Pathology, Lineberger Comprehensive Cancer Center, The University of North Carolina at Chapel Hill, Chapel Hill, NC 27599, USA
[8]Laboratory of Cell Regulation and Carcinogenesis, National Cancer Institute, Bethesda, MD 20892, USA
[9]These authors contributed equally to this work.
[10]Present address: Center for Cancer Research, Massachusetts General Hospital, Boston, MA 02414, USA.
[11]Present address: Lee Gil Ya Cancer and Diabetes Institute, Gachon University of Medicine and Science, Songdo, Incheon 406-840, Korea.
*Correspondence: stuart_orkin@dfci.harvard.edu
DOI 10.1016/j.ccr.2007.11.012

## SUMMARY

**To better understand the cellular origin of breast cancer, we developed a mouse model that recapitulates expression of the ETV6-NTRK3 (EN) fusion oncoprotein, the product of the t(12;15)(p13;q25) translocation characteristic of human secretory breast carcinoma. Activation of EN expression in mammary tissues by *Wap-Cre* leads to fully penetrant, multifocal malignant breast cancer with short latency. We provide genetic evidence that, in nulliparous *Wap-Cre;EN* females, committed alveolar bipotent or CD61$^+$ luminal progenitors are targets of tumorigenesis. Furthermore, EN transforms these otherwise transient progenitors through activation of the AP1 complex. Given the increasing relevance of chromosomal translocations in epithelial cancers, such mice serve as a paradigm for the study of their genetic pathogenesis and cellular origins, and generation of preclinical models.**

## INTRODUCTION

For most malignancies neither the initiating genetic event nor the cell of origin is known. Cancers are heterogeneous in composition and are organized in a hierarchy that includes cells competent to recreate the tumor on transplantation, designated tumor initiating cells (T-ICs) or cancer stem cells, and other cells comprising the bulk tumor mass (Reya et al., 2001). Following the first hit, whether it occurs within a stem or more differentiated cell, secondary events of genetic or epigenetic nature contribute to evolution of malignancy. Access to these early steps in

## SIGNIFICANCE

For the largest class of human tumors, those of epithelial origin, little is known about their initiating genetic hits or cells of origin. Whether tissue stem cells or more committed progenitors are targets for transformation is uncertain. We developed a system in which epithelial tumorigenesis can be assessed from the initial event to frank malignancy. In this breast cancer model based on chromosomal translocation, we show through genetic marking that committed mammary progenitors, rather than mammary stem cells, are direct targets of transformation. We show that activation of the AP1 complex represents a critical downstream event of the ETV6-NTRK3 translocation. Further focus on this transcriptional complex as a target in human breast cancer is warranted.

cancer formation is impossible in patients. Animal models provide a window into this phase of cancer development but are likely to be relevant to human biology only so far as the genetic events mirror those occurring in patients.

In considering these issues, we have sought to apply to a cancer of epithelial origin principles that have proved successful in the study of hematopoietic malignancies. For leukemias and childhood sarcomas, chromosomal translocations leading to the production of chimeric proteins serve as initiating genetic events (Rowley, 2001). Although some gene rearrangements associated with leukemia are rare, study of these infrequent events has defined transcription factors critical for normal differentiation and pathways more generally perturbed in malignancy.

Until lately, the contribution of chromosomal rearrangements to epithelial cancers has been viewed as minor. Recently, chromosomal rearrangements involving the ETS family transcription factors were identified in >50% cases of human prostate cancer (Tomlins et al., 2005, 2006, 2007). Furthermore, an *EML4-ALK* fusion gene was identified in 6.7% of non-small-cell lung cancer cases (Soda et al., 2007). These observations prompt reassessment of conclusions regarding the involvement of chromosomal rearrangements in epithelial cancer.

t(12;15)(p13;q25) is a unique recurrent chromosomal translocation associated with cancer of all germ layers, including human secretory breast carcinoma (SBC) (Tognon et al., 2002), congenital fibrosarcoma (Knezevich et al., 1998b), congenital mesoblastic nephroma (Knezevich et al., 1998a; Rubin et al., 1998), and acute myelogenous leukemia (Eguchi et al., 1999). It produces a fusion oncogene, *ETV6-NTRK3* (*EN*), which encodes a chimeric protein made up of the oligomerization domain of ETV6 (also known as TEL, an ETS family transcription factor) and the protein tyrosine kinase (PTK) domain of NTRK3 (also known as TRKC, a TRK family tyrosine kinase receptor for neurotrophin-3). The consistent presence of this translocation in human SBC provides strong genetic epidemiological support for its role in the initiation of breast cancer (Tognon et al., 2002).

Breast cancer is representative of other epithelial malignancies in its heterogeneity, both genetically and clinically (Simpson et al., 2005). In part, phenotypic heterogeneity may reflect diverse cellular origins of different subtypes of breast cancer (Ince et al., 2007).

Here we report a murine model of human sporadic breast cancer based on the *EN* translocation. We demonstrate that two committed mammary progenitors in the normal mammary developmental hierarchy serve as target cells of breast cancer. In addition, by performing microarray analysis, we reveal that EN-initiated transformation is mediated largely through activation of the c-Jun/Fosl1 AP1 complex.

## RESULTS

### Generating the *Etv6-NTRK3* Conditional Knockin Allele

We generated a Cre-Lox *EN* knockin allele by introducing the portion of human *NTRK3* cDNA encoding the PTK domain (as found in SBC patients) into exon 6 of the mouse *Etv6* locus (Figure 1A). We rendered this fusion allele conditional by insertion of a "floxed" transcriptional terminator sequence ("stopper" [Mao et al., 1999]; Figure 1A] into the intron upstream of the knockin *NTRK3* cDNA. The resulting allele, once activated by Cre-mediated excision of the floxed "stopper," produces a mouse Etv6-human NTRK3 hybrid protein, which transforms NIH 3T3 cells (data not shown). Therefore, the *EN* knockin allele recapitulates the chimeric protein seen in patients.

We identified correctly targeted ES cell clones using Southern blot (Figure 1B). By RT-PCR, we found *EN* ES cells without excision exhibited slightly leaky expression of the *EN* allele, but removal of the "stopper" greatly increased its expression (Figure 1C). At the protein level (Figure 1D), no EN fusion protein was detected in unexcised ES cells. However, its expression was readily visible from "stopper"-excised ES cells. Thus, the *EN* conditional knockin allele functions as designed.

### The Endogenous *Etv6* Locus Is Active in Mammary Epithelial Cells

Because *EN* is under the control of the endogenous *Etv6* promoter, we first examined where *Etv6* is normally expressed in mammary glands (MGs) using a mouse strain we generated (TEA175) that carries an *Etv6* locus having a β-Geo cassette inserted between its exons 2 and 3 and serves as a reporter for its expression.

Upon staining MGs from TEA175 heterozygous females for *lacZ* activity, we found that *Etv6* is expressed in both ductal and alveolar mammary epithelial cells (MECs) (Figure S1A in the Supplemental Data available with this article online). In addition, flow cytometry analysis revealed *lacZ*$^+$ cells in all four major MEC subpopulations defined previously (Stingl et al., 2006) (Figure S1B).

### Activation of *EN* in Mammary Glands by *Wap-Cre* Leads to Mammary Tumors with Complete Penetrance

Without Cre-mediated activation of *EN*, heterozygotes were indistinguishable from their wild-type (WT) littermates. Some *EN* heterozygous females (and very rarely, males) developed mammary tumors at advanced ages (>1 year), possibly due to the leakiness of the "stopper" and low-level EN expression (Figure 1C).

To activate *EN* expression in MGs, we initially planned to use two commonly used MG-specific Cre mouse lines, *MMTV-Cre* and *Wap-Cre* (Wagner et al., 1997). Unfortunately, use of *MMTV-Cre* led to a lethal myeloproliferative disease within several weeks after birth, apparently due to expression of *MMTV-Cre* in the hematopoietic system (data not shown).

The more restricted expression of the endogenous *Wap* gene as well as that of the *Wap-Cre* transgene (Boulanger et al., 2005; Kordon et al., 1995; Robinson et al., 1995, 1996; Wagner et al., 2002) afforded an approach for activation of *EN* in MGs without accompanying effects in other tissues. In maturing and mature nulliparous female mice, *Wap*$^+$ cells are present only

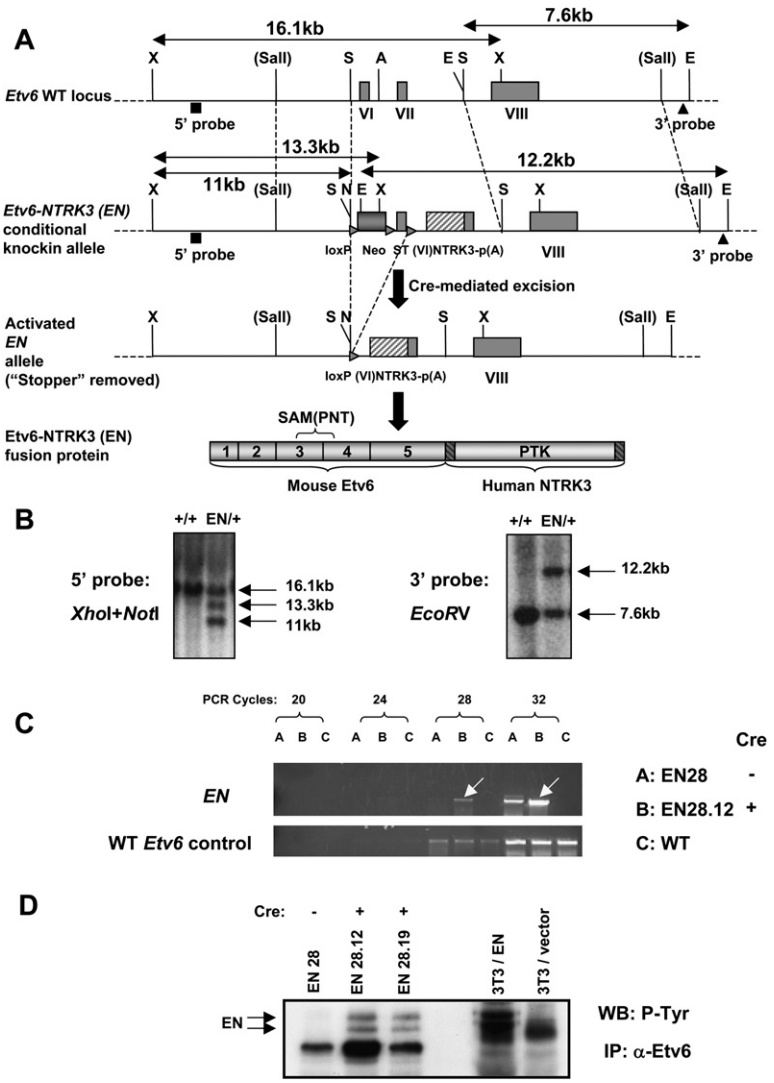


**Figure 1. Generating the *Etv6-NTRK3* Conditional Knockin Allele**

(A) Schematic diagrams of the endogenous WT *Etv6* allele, the *Etv6-NTRK3* (*EN*) conditional knockin allele, the activated *EN* allele upon Cre-mediated excision of the floxed *Neo-stopper* cassette (ST, stopper), and the EN fusion protein produced from the activated *EN* allele. The 5′ and 3′ probes for Southern blot are shown. X, XhoI; S, SpeI; A, ApaI; E, EcoRV; N, NotI; VI, VII, VIII, exon 6, 7, and 8 of *Etv6*; p(A), poly(A) signal; SAM(PNT), sterile alpha motif/pointed domain; PTK, protein tyrosine kinase domain.

(B) Southern blot screen and confirmation of correctly targeted ES cell clones. The 5′ probe recognizes a 16.1 kb XhoI fragment from the WT *Etv6* allele, a 13.3 kb XhoI fragment (due to incomplete digestion of NotI) and an 11 kb XhoI-NotI fragment (complete digestion) from the *EN* knockin allele. The 3′ probe recognizes a 7.6 kb EcoRV fragment from the WT allele, and a 12.2 kb EcoRV fragment from the *EN* allele.

(C) RT-PCR analysis showing greatly elevated expression of the *EN* fusion transcript from the "stopper"-excised ES cells (EN28.12). Note that *EN* has slightly leaky expression in the parental EN28 ES cells (without excision of the "stopper").

(D) Western blot showing detection of the EN fusion protein (tyrosine phosphorylated doublet) from the "stopper"-excised ES cells (EN28.12, EN28.19), but not from the parental EN28 ES cells. EN-3T3 cells were used as the positive control.

transiently as a minor subset at estrus. *Wap* expression is greatly elevated in differentiating MECs during late pregnancy and lactation and then turned down following involution.

Based on the expression pattern of *Wap*, we initially predicted that *Wap-Cre;EN* (hereafter, *WCEN*) female mice might require rounds of pregnancies in order to express sufficient Cre to activate *EN*. Unexpectedly, however, all nulliparous *WCEN* females develop multifocal mammary tumors as early as 4 months of age (Figure 2A), with preceding lobuloalveolar hyperplasia (Figure 2B). Parous *WCEN* females develop similar multifocal mammary tumors with antecedent alveolar hyperplasia, and with no significant differences in tumor latency and histology. Some aged *WCEN* males also develop mammary tumors (Figure 2A and data not shown).

To confirm that mammary tumors in *WCEN* animals resulted from activation of *EN* expression, we performed PCR analysis on genomic DNA prepared from tumors and other organs of *WCEN* animals and found that the "stopper" in the *EN* allele was excised only in tumor cells (Figure 2C). Consistent with this, we also detected EN protein in tumor tissues by western blot (Figure 2D). Previous studies demonstrated that expression of the EN fusion protein in 3T3 cells led to constitutive phosphorylation of Mek1/2 and Akt as well as to a constitutive high-level expression of cyclin D1/2 (Tognon et al., 2001). These features also characterized EN-initiated mammary tumors (hereafter, EN tumors) (Figure 2D).

EN tumors were heterogeneous both with respect to morphology and rate of tumor progression (Figures 2Ea–2Ed and data not shown). Most EN tumors were highly invasive and transplantable upon subcutaneous injection into immunodeficient mice. The rate of tumor regrowth following transplantation correlated with the apparent rate of progression of the corresponding primary tumor. Due to the relatively short latency of these tumors, most *WCEN* mice failed to show signs of metastasis. On occasion, metastases to lymph node and lung were observed (Figures 2Ef and 2Eh).

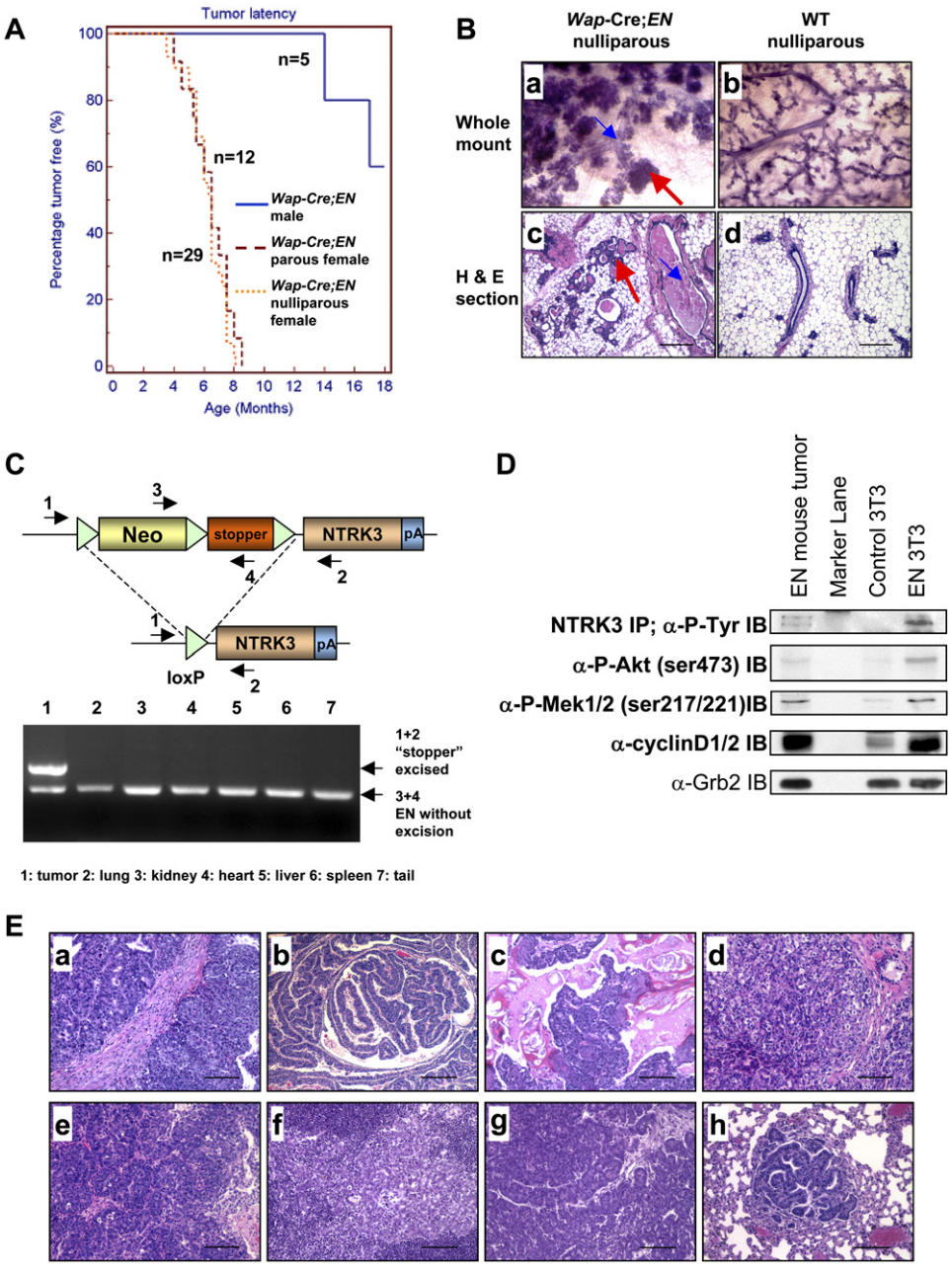


**Figure 2. *Wap-Cre;EN* Mice Develop Mammary Tumors with Antecedent Alveolar Hyperplasia**

(A) Tumor-free curves.

(B) Mammary glands (MGs) of *WCEN* females (Ba and Bc) exhibit extensive lobuloalveolar hyperplasia compared to WT (Bb and Bd). (Ba and Bb) MG whole mounts stained with hematoxylin. (Bc and Bd) Hematoxylin & eosin (H&E)-stained MG sections (scale bars, 200 μm). Red arrows: alveolar hyperplasia. Blue arrows: dilated ducts and accumulation of secretions within ducts.

(C) PCR analysis on genomic DNA shows excision of the *Neo-stopper* cassette only in the tumor. Locations of PCR primers (1–4) are indicated.

(D) Western blot analysis of the *WCEN* tumor. EN-3T3 cells were used as the positive control. IP/western confirms EN expression in both the tumor and EN-3T3 cells.

(E) Histology (H&E-stained sections; scale bars, 100 μm) of mammary tumors developed in *WCEN* mice. (Ec) shows squamous metaplasia, (Ee) and (Ef) were from a nulliparous female, (Ee) shows a primary mammary tumor, and (Ef) shows metastasis in a lymph node; (Eg) and (Eh) were from a male, (Eg) shows a primary mammary tumor, and (Eh) shows metastasis in the lung.

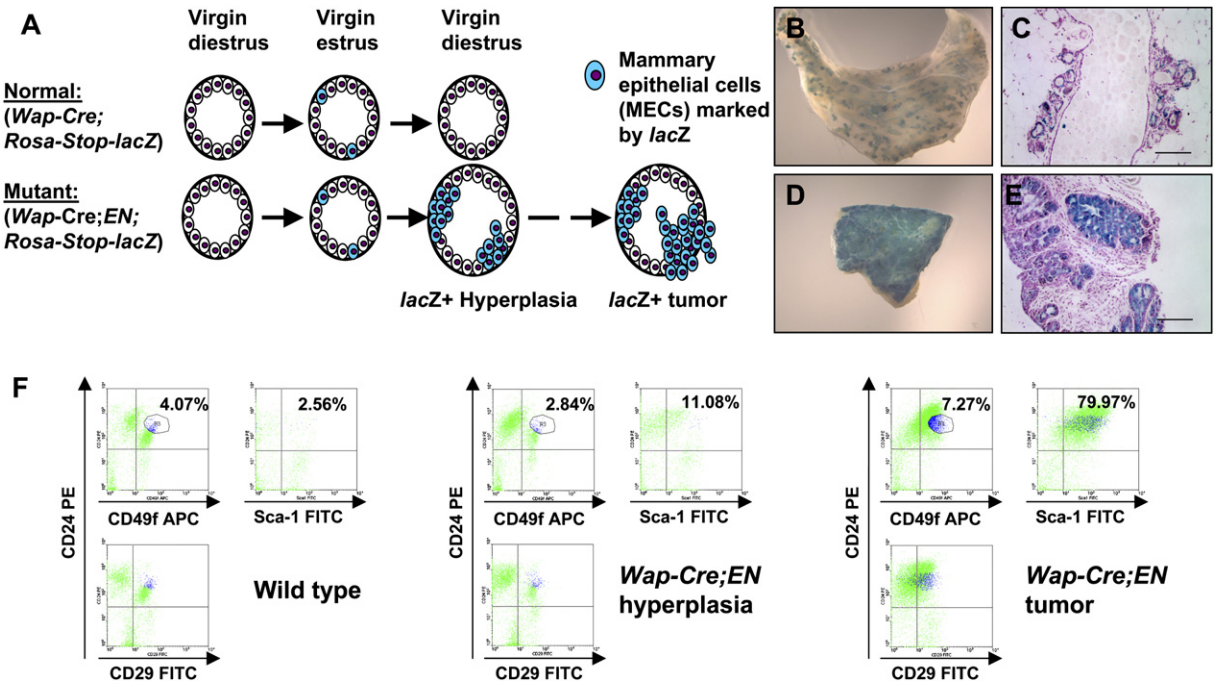


**Figure 3. Target Cells of Mammary Tumors Developed in *Wap-Cre;EN* Virgins Are Transient Mammary Progenitors, Rather Than MaSCs**

(A) Schematic diagram of the *lac*Z-marking experiment. Normal *WCLZ* virgin MGs contain a transient wave of *lacZ*$^+$ MECs. In *WCENLZ* mutant MGs, the transient *lacZ*$^+$ MECs appear to be rescued from death and lead to *lacZ*$^+$ alveolar hyperplasia and eventually *lacZ*$^+$ mammary tumors.

(B–E) (B) and (D) show whole mounts of *WCENLZ* MG and tumor stained for *lac*Z activity. (C) and (E) are *lacZ*-stained tissue sections counterstained with nuclear fast red. Note that, in (B) and (C), *lacZ*$^+$ cells are mainly restricted to the alveolar compartment. Scale bars, 100 μm.

(F) Flow cytometry analysis of a WT MG, a *WCEN* hyperplastic MG, and a *WCEN* tumor. The profiles shown here have already been gated for lineage-negative (Lin$^-$) cells. Percentages of positive cells are from a representative experiment.

## The Transient *Wap*$^+$ Cells in Nulliparous *Wap-Cre;EN* Mammary Glands Are Target Cells of EN

In nulliparous female mice, *Wap* is activated in a small, transient population of MECs during estrus (Kordon et al., 1995; Robinson et al., 1995, 1996). Further studies in *Wap-Cre;Rosa-Stop-lacZ* (hereafter, *WCLZ*) females showed that *Wap-Cre*$^+$ (thus also *lacZ*$^+$) MECs failed to persist in *WCLZ* mice during diestrus. Since *lacZ*$^+$ cells do not accumulate in nulliparous *WCLZ* mice, it is inferred that the MECs in which *Wap* is first activated do not proliferate extensively and possibly die through apoptosis (Boulanger et al., 2005; Henry et al., 2004; Wagner et al., 2002). In addition, one can infer that *Wap-Cre*$^+$ cells are not equivalent to mammary stem cells (MaSCs) in virgin mice.

Since *WCEN* nulliparous females develop multifocal mammary tumors with 100% penetrance and the transient *Wap*$^+$ MECs are likely the only cells in virgins that express Cre and, therefore, activate *EN* expression, we conjectured that these cells might be direct targets of EN transformation (Figure 3A). To test this hypothesis, we interbred a *Rosa-Stop-lacZ* reporter (Mao et al., 1999) into the *WCEN* background and generated *Wap-Cre;EN;Rosa-Stop-lacZ* (hereafter, *WCENLZ*) females. We predicted the presence of *lacZ*$^+$ hyperplastic MECs in MGs and subsequent development of *lacZ*$^+$ mammary tumors (Figure 3A). Indeed, *lac*Z staining was primarily restricted to hyperplastic alveolar cells in hyperplastic MGs (Figures 3B and 3C). Moreover, *lacZ*$^+$ cells were confined to tumor epithelial cells in mammary tumors (Figures 3D and 3E). Thus, genetic marking suggests that activation of *EN* by Cre rescues an otherwise transient subpopulation of MECs and maintains them and their progeny for subsequent steps in progression to frank malignancy. Furthermore, we reasoned that T-ICs in *WCENLZ* tumors should also be marked by *lac*Z. To test this, we transplanted tumor cells into immunodeficient mice after limited dilutions. Without fractionation, typically $\sim 10^4$–$10^5$ EN tumor cells were needed to form new tumors in *Rag2*$^{-/-}$ mice. In contrast, only $\sim 10^3$–$10^4$ (sometimes even as low as 600) sorted *lacZ*$^+$ tumor cells were sufficient to initiate new tumors in *Rag2*$^{-/-}$ hosts. This suggests that T-ICs, evolved from EN target cells, are enriched in the population of *lac*Z-marked EN tumor cells.

## *Wap-Cre;EN* Hyperplastic Mammary Glands and Tumors Accumulate CD24$^+$Sca-1$^+$ Cells

To characterize further the nature of the EN target cells, we examined surface markers that have previously been used to fractionate mammary tissues into enriched stem or progenitor populations (Shackleton et al., 2006; Stingl et al., 2006; Welm et al., 2002). By flow cytometry analysis, most EN tumor cells were CD24$^+$Sca-1$^+$ (Figure 3F).

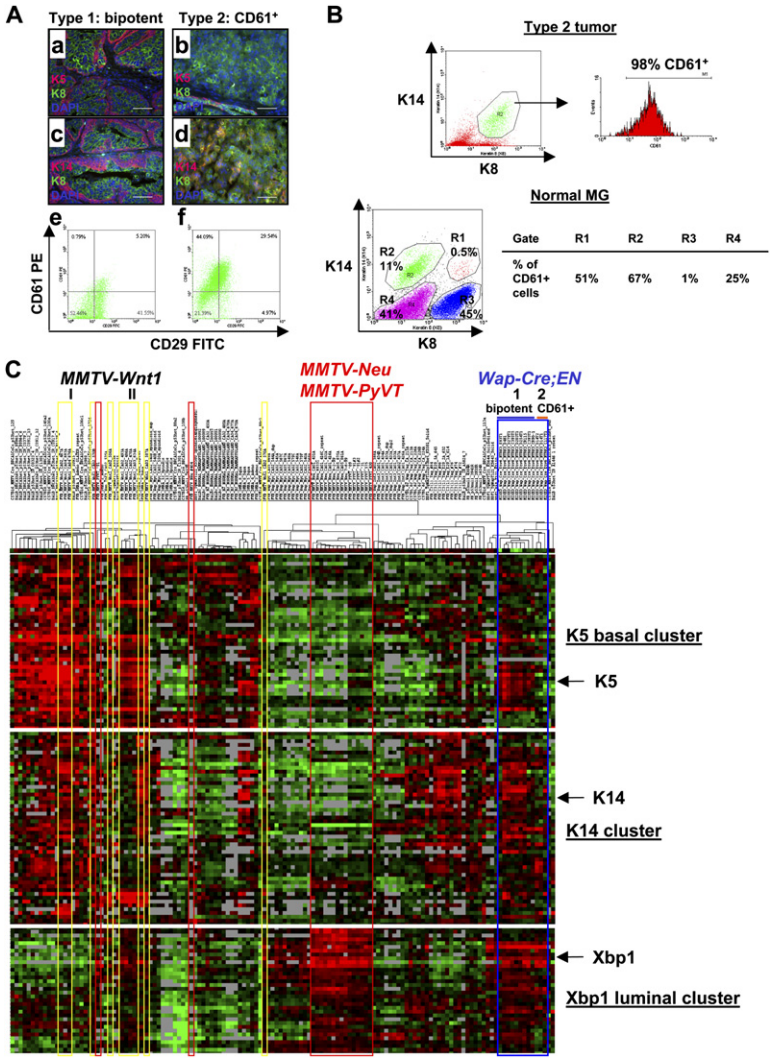


**Figure 4. Two Major Types of *Wap-Cre;EN* Tumors Characterized by Immunostaining and Microarray Analysis**

(A) EN type 1 (bipotent: [Aa], [Ac], and [Ae]) and type 2 (CD61$^+$: [Ab], [Ad], and [Af]) tumors based on K5/K8 (Aa and Ab), K14/K8 (Ac and Ad), and CD61/CD29 (Ae and Af) staining patterns. Scale bars, 50 μm.

(B) Flow cytometry analysis showing that K8$^+$K14$^+$ cells in EN type 2 tumors are CD61$^+$. In normal MGs, almost all CD61$^+$ MECs (gates R1–R3) are K14$^+$. Gate R4 represents nonepithelial cells in MGs.

(C) Hierarchical cluster analysis of 12 *WCEN* tumors (type 1 and 2, blue lines) together with 122 samples from other murine models of breast cancer and normal MGs. *MMTV-Wnt1* tumors (clusters I and II) are highlighted by yellow lines. *MMTV-Neu* and *MMTV-PyVT* tumors are highlighted by red lines. Heat maps of three representative gene clusters (*K5*, *K14*, and *Xbp1*) are shown (heat maps showing all genes in the intrinsic gene list are shown in Figure S5). Gene names for each cluster are listed in Table S8. In the heat map, red, black, and green represent above average, average, and below average levels of expression, respectively. Gray indicates no data recorded.

Moreover, MGs from mature nulliparous *WCEN* females contained a greater number of CD24$^+$Sca-1$^+$ cells than WT controls even before they developed tumors (Figure 3F). In contrast, the MaSC-enriched Lin$^-$CD29$^{hi}$CD24$^+$ (Shackleton et al., 2006; and the similar Lin$^-$CD49f$^{hi}$CD24$^+$ [Stingl et al., 2006]) subpopulation is not altered in *WCEN* hyperplastic MGs (Figure 3F). These data argue that mammary tumors in *WCEN* mice are unlikely to arise from transformation of MaSCs; instead, they may be derived from committed CD24$^+$Sca-1$^+$ mammary progenitors.

## *Wap-Cre;EN* Mammary Tumors Are Derived from Committed Alveolar Progenitors

In analogy to the hematopoietic system, a developmental hierarchy for MECs, including MaSCs, bipotent ductal or alveolar progenitors, single lineage-restricted progenitors, and mature luminal or myoepithelial cells, has been proposed (Asselin-Labat et al., 2007; Hennighausen and Robinson, 2005). To position target cells of EN in this hierarchy, we performed immunostaining for the luminal epithelial cell marker keratin 8 (K8), basal/myoepithelial cell markers keratin 5 (K5) and 14 (K14), p63, and α-smooth muscle actin (SMA), as well as the mammary progenitor marker keratin 6 (K6), and estrogen receptor (ERα) (Figure 4A and Figure S2). Overall, we have identified two broad tumor types in *WCEN* mice. The majority of EN tumors (type 1, ~90%) exhibit relatively well-differentiated glandular structures and contain K8$^+$ luminal epithelial cells surrounded by basal/myoepithelial cells that are positive for K5, K14, p63, and sometimes, SMA. Occasionally there are K5$^+$K14$^+$p63$^+$SMA$^{+or-}$ basal/myoepithelial cells "leaking" into the region of luminal epithelial cells (Figure 4A and Figures S2A and S2D). In the most extreme case, some type 1 tumors (type 1a, or regions within these tumors) contain a large number of K5$^+$K14$^+$p63$^+$SMA$^{+or-}$ basal/myoepithelial cells intermixed with a smaller number of K8$^+$ luminal epithelial cells in a less organized manner (Figure S2A). A second class of EN tumors (type 2, ~10%) exhibits no K5$^+$K14$^+$p63$^+$ basal/myoepithelial cells but contains predominantly K8$^+$ luminal epithelial cells. Interestingly, a large number of K8$^+$ cells in these tumors are also K14$^+$ (but K5$^-$)

(Figure 4A and Figure S2A). In contrast, most type 1 tumors lack these abnormal $K8^+K14^+$ cells. However, some type 1a tumors do contain a small number of $K8^+K14^+$ cells (Figure S2A). In addition, we also identified an additional subtype of type 1 tumors (type 1b) that exhibit glandular structures, with $K8^+$ luminal epithelial cells surrounded by $K5^+K14^+$ basal/myoepithelial cells. However, many of these $K8^+$ luminal cells are also $K14^+$ (Figure S2A), thus representing tumors with features of both types (1 and 2). A summary of the staining properties of cells in the different types of EN tumors is provided in Figure S2B. The majority of type 1 tumors contain K6-expressing cells, whereas very few or no $K6^+$ cells are present in type 2 tumors (Figure S2C). However, tumors of both types express Sca-1 (data not shown) and are $ER\alpha^+$ (Figure S2E). Interestingly, upon careful examination by immunofluorescence colocalization, we observed a significant number of $ER\alpha^+p63^+$ and $ER\alpha^+SMA^+$ cells, in addition to the $ER\alpha^+p63^-SMA^-$ luminal epithelial cells (Figure S2E).

Recently, CD61 (integrin β3) has been shown to mark the luminal progenitors in normal MGs (Asselin-Labat et al., 2007). Interestingly, we find that all type 2 tumors abundantly express CD61, whereas most of the type 1 tumors contain much fewer $CD61^+$ cells (Figures 4Ae and 4Af), with the exception of type 1b tumors. Microarray expression profiling confirms that type 2 tumors express the highest levels of CD61, followed by type 1b, and then the remaining type 1 tumors (data not shown). Since type 2 tumors exhibit "luminal" appearance and are characterized by large numbers of $K8^+K14^+$ cells, we asked whether these double-positive cells might represent blocked $CD61^+$ progenitors. In fact, flow cytometry analysis revealed that almost all $K8^+K14^+$ cells in these tumors are $CD61^+$ (Figure 4B). In normal MGs, the majority of $CD61^+$ cells are $K8^-K14^+$ cells, whereas $K8^+K14^-$ luminal cells are $CD61^-$ (Figure 4B). We also detected a small population of $K8^+K14^+$ cells, a significant number of which also express CD61 (Figure 4B). These data suggest that $CD61^+$ luminal progenitors are K14-expressing cells, and the abnormal $K8^+K14^+$ cells in EN type 2/type 1b tumors probably represent $CD61^+$ luminal progenitors blocked in differentiation toward $K8^+K14^-$ mature luminal epithelial cells.

In type 1 EN tumors, the $K5^+$ basal/myoepithelial cells, in addition to the $K8^+$ luminal cells, are part of the tumor epithelial cell population. When we compared microarray expression profiles generated from sorted tumor epithelial cells based on the above-described *lac*Z marker in *WCENLZ* females to those from unfractionated tumors, we observed slight enrichment (rather than loss) of both the *K5* basal gene cluster and the *K14* cluster (as defined in Figure 4C, discussed below) in sorted *lac*$Z^+$ tumor cells, as determined by gene set enrichment assay (GSEA) (data not shown) (Subramanian et al., 2005). This confirms that basal/myoepithelial cells in EN tumors are part of the tumor epithelial cells, not normal cells recruited to tumors.

Due to the presence of mixed cell types in type 1 EN tumors, the cells from which tumors originate could be MaSCs, bipotent progenitors, or multiple lineage-committed progenitors. Since the above-described genetic marking experiment and flow cytometry analysis (Figure 3) both rule out MaSCs as targets of EN, we next asked whether tumors are derived from *distinct* lineage-restricted progenitors (i.e., multiclonal), or from bipotent progenitors (i.e., clonal).

We used a *Wap-rtTA-Cre* transgenic line that expressed Cre in *Wap*$^+$ cells in the presence of doxycycline (Utomo et al., 1999). We generated animals with both *Wap-rtTA-Cre* and *EN*, some of which also carried a conditional luciferase reporter at the *Rosa26* locus (*Rosa-Stop-Luc*, similar to the above-described *Rosa-Stop-lac*Z reporter [Safran et al., 2003]). Unexpectedly, we found that the *Wap-rtTA-Cre* transgene exhibits leaky Cre expression, and *Wap-rtTA-Cre;EN* nulliparous females developed mammary tumors without doxycycline. These tumors also featured cells of both luminal and basal/myoepithelial lineages (Figure S3A). Since Cre should be expressed at a low level without doxycycline, sometimes it might excise the "stopper" at the *EN* allele but not that at the *Rosa-Stop-Luc* allele within the same cell. If a tumor arose from a cell with this genotype, tumor epithelial cells would all inherit the recombined *EN* allele and the unmodified *Rosa-Stop-Luc* allele. Indeed, in a tumor arising in a *Wap-rtTA-Cre;EN;Rosa-Stop-Luc* nulliparous female, we detected excision only at the *EN* locus, and not at the *Rosa-Stop-Luc* locus (Figure S3B). Since it is highly unlikely for multiple lineage-restricted progenitors to obtain the same partial excision pattern (as described above) and then give rise to a tumor with this pattern, our observation supports the clonal origin of type 1 EN tumors from bipotent progenitors.

Furthermore, microarray data reveal that, compared to normal MGs, both type 1 and 2 EN tumors express high levels of the alveolar cell marker κ-casein, but low levels of the ductal cell marker NKCC1 (also known as "solute carrier family 12, member 2") (Figure S4A), suggesting an alveolar cellular origin. In contrast, *MMTV-Wnt1* tumors do not express (or express low levels of) κ-casein but express NKCC1 in a fraction of tumor cells, consistent with MaSCs as potential target cells to give rise to both ductal and/or alveolar cells (Li and Rosen, 2005) (Figure S4B). Taken together, we conclude that target cells of mammary tumors arising in *WCEN* females are either committed bipotent alveolar progenitors (type 1) or luminal alveolar progenitors (type 2). These progenitors are within the transient *Wap*$^+$ cells in nulliparous females.

### *Wap-Cre;EN* Mammary Tumors Express Both Luminal and Basal Gene Clusters

We compared EN tumors to other murine breast cancer models by microarray expression profiling, using hierarchical clustering based on an intrinsic gene list developed for murine models of breast cancer (Herschkowitz et al., 2007). As shown in Figure 4C and Figure S5, in general, compared to other murine models, EN tumors are relatively homogeneous and cluster together. However, the 3 type 2 tumors (D14T1, D14T2, and C117T1) form their own subcluster and are separated from the type 1 tumors. In contrast, tumors from parous (CR115, CR90-1, D14T1,

and D14T2) and nulliparous (the remaining samples) females are mixed together and do not form distinct subclusters. These data suggest that the initiating oncogenic event and cellular origin, but not the reproductive history, are more important in determining phenotypes of EN tumors.

All type 1 EN tumors express 3 gene clusters, including a *K5* basal gene cluster, a strong *K14* cluster, and a strong *Xbp1* luminal gene cluster, similar to *MMTV-Wnt1* tumors (Figure 4C). Type 2 EN tumors express the *K14* and *Xbp1* clusters, but not the *K5* cluster. In contrast, tumors from both *MMTV-Neu* and *MMTV-PyVT* mice only express the *Xbp1* luminal cluster (Figure 4C). Of note, *MMTV-Wnt1* tumors are more heterogeneous than EN tumors and they can also be divided into two major subclusters. One contains *K5* and *K14* clusters, but not the *Xbp1* luminal cluster (Figure 4C, cluster I). The other contains the *K5* basal cluster and the *Xbp1* luminal cluster (though expressed at slightly lower levels), but not the *K14* cluster (Figure 4C, cluster II). These differences may be due in part to their different cells of origin, with MaSCs as more likely targets of *MMTV-Wnt1* tumors, and committed progenitors as targets of EN.

## An AP1 Signature Associated with EN-Mediated Mammary Tumorigenesis

To understand the mechanism of EN-mediated mammary tumorigenesis, we first performed GSEA on microarray expression profiles from unsorted EN tumors compared to those from normal MGs, using curated gene sets (c2 collection) for metabolic and signaling pathways from the GSEA molecular signature database website (http://www.broad.mit.edu/gsea/msigdb/msigdb_index.html). Unexpectedly, this analysis only revealed pathways that seem to be common for tumor cells in general (e.g., reflecting increased metabolic activities and proliferation; Table S1). Two possibilities may account for this result. First, pathways that are active in both normal MGs and tumors may not be revealed by this assay. Second, noncancerous cells in these tumors could introduce significant "noise" in unsorted tumor samples.

In our *WCENLZ* animals, tumor epithelial cells are labeled by *lacZ* (Figures 3B–3E). Thus, we have the opportunity to mark tumor epithelial cells and separate them from stromal cells. In addition, target cells of EN in *WCLZ* virgin females as well as premalignant, hyperplastic MECs in *WCENLZ* females are also marked by *lacZ*, thus providing an opportunity to isolate these cells for analysis.

We generated microarray expression profiles for several *lacZ*-sorted samples from either *WCENLZ* hyperplastic MGs that had not developed visible tumors, or mammary tumors that arose in *WCENLZ* females. We then compared sorted tumor cells to sorted hyperplastic MECs by GSEA using the above-described c2 gene sets, in an attempt to identify pathways upregulated during tumor progression. The top gene sets enriched in sorted tumor cells derived from this comparison are more informative than the comparison using unsorted tumors (Table S2, compare to Table S1). Pathways related to the hypoxia response in tumors, WNT signaling, TRK/NGF signaling, TGFβ signaling, and genes regulated by MYC are evident. To further validate the effectiveness of this approach, we also compared unsorted tumors to sorted hyperplastic MECs (thus both comparisons have the same baseline). The top gene sets enriched in unsorted tumors revealed from this analysis are very similar to those compared to normal MGs (Table S3, compare to Table S1), suggesting that GSEA using sorted tumor cells may reveal pathways with better specificity than using unsorted tumors.

We next compared sorted tumor cells to unsorted tumors by GSEA using c2 gene sets. We reasoned that genes/pathways upregulated specifically in tumor epithelial cells would be further enriched in this comparison. This would also potentially reveal an overall EN "signature" in the tumor epithelial cell compartment composed of pathways upregulated during the initial transformation, or tumor progression, or both. Among gene sets enriched in sorted tumor cells, we observed pathways related to genes regulated by C/EBP, IL6 response, HOXA5 targets, WNT signaling, JNK signaling, and TGFβ signaling (Table S4).

To determine what portion of the EN tumor signature is acquired during tumor initiation, ideally we would need to sort normal target cells of EN and compare their expression profiles to those from sorted hyperplastic MECs. Unfortunately, *lacZ* staining of mammary tissues by FDG dye yields a significant amount of background staining (~1%–3% even for *lacZ*$^-$ tissues). This background staining does not cause difficulty when sorting *lacZ*$^+$ hyperplastic MECs or tumor cells, which typically constitute ~10%–40% of total cells, but prohibits sorting the small population of transient EN target cells (0.8%–4% as estimated by Wagner et al. [Wagner and Smith, 2005]) with sufficient confidence. To overcome this technical limitation, we turned to an in vitro model of EN signaling. Because EN is a unique oncoprotein in that it transforms cells of all germ layers, we reasoned that the mechanism of EN-mediated transformation might be conserved in different cell types. EN-mediated signaling in NIH 3T3 cells has been studied previously (Tognon et al., 2001; Wai et al., 2000), many of which were also observed in EN tumors (Figure 2D). Thus, we generated microarray expression profiles from EN-transduced 3T3 cells (EN-3T3) and compared them to those of untransformed 3T3 cells. By performing GSEA using c2 gene sets, we identified several common gene sets that are enriched in both EN-3T3 cells and sorted EN tumor cells, including 2 IL6 pathways, "WNT_TARGETS," "CHEN_HOXA5_TARGETS_UP," and "TGF_BETA_SIGNALING_PATHWAY" (Table S5, compare to Table S4).

Since "WNT_TARGETS" arose among the top-enriched gene sets in all three analyses, we next focused on this gene set. By comparing the core enrichment genes from all three analyses, we observed striking similarity between sorted tumor cells (compared to unsorted tumors) and EN-3T3 cells (compared to control 3T3 cells) (Figures S6A and S6B), including genes such as *JUN*, *FOSL1*, *PLAUR*, and *CD44*. *JUN* and *FOSL1* (also known as *FRA1*) encode components of the AP1 complex and are target genes of

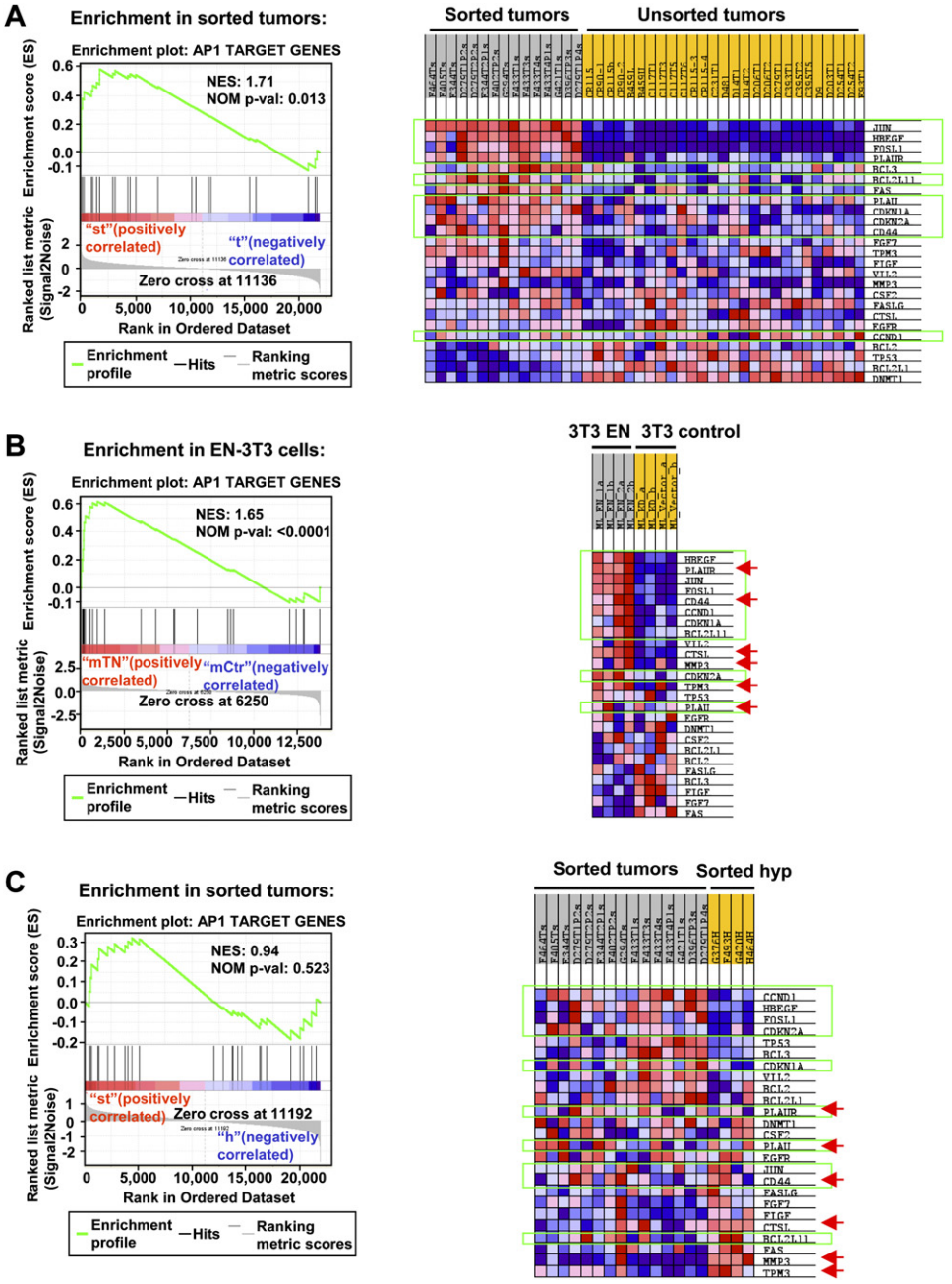


**Figure 5. Enrichment of c-Jun/Fosl1 and AP1 Targets in EN-Transformed Cells**

(A–C) GSEAs show enrichment of c-Jun/Fosl1 and AP1 target genes in sorted EN tumor cells compared to unsorted tumors (A) and sorted hyperplastic cells (C), and in EN-3T3 cells (B). Genes expressed at higher levels in both sorted tumors and EN-3T3 cells are highlighted with green lines. Genes expressed at higher levels in both sorted hyperplastic MECs and EN-3T3 cells are indicated by red arrows.

β-catenin in human colorectal carcinomas. *PLAUR* encodes uPAR, and its transcription is activated through AP1 (Mann et al., 1999). In addition, CD44 can also be upregulated by AP1 activity (Lamb et al., 1997). Thus, this four-gene set appears to represent an AP1 signature.

Consistent with the above data, we also observed enrichment of all gene sets containing genes with the AP1-binding motif in the c3 collection of GSEA database in sorted tumor cells and EN-3T3 cells (Table S6). More directly, we manually compiled a gene set for AP1 target genes based on published literature (plus *JUN* and *FOSL1*) (Eferl and Wagner, 2003) and observed its significant enrichment in both sorted EN tumor cells and EN-3T3 cells (Figures 5A and 5B). In addition to the above-described four-gene set, we identified additional AP1 target genes that are upregulated in both comparisons, including

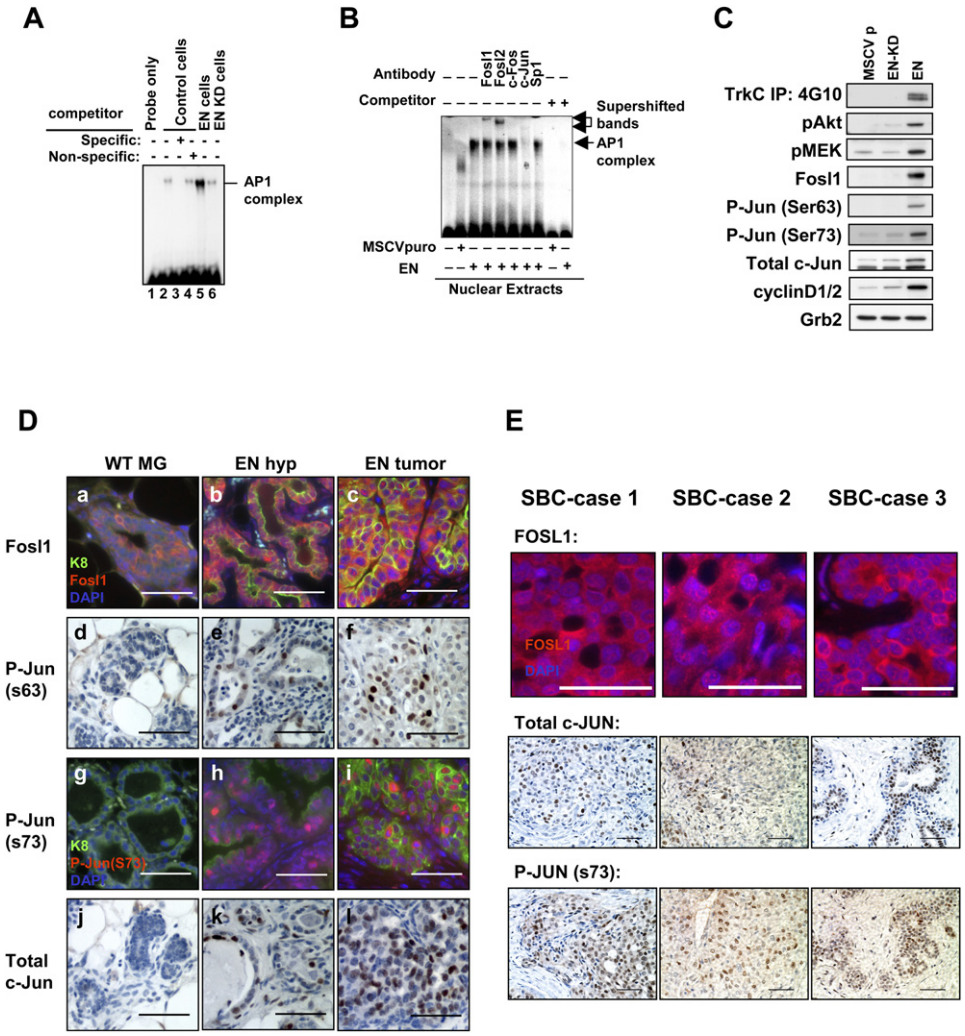


**Figure 6. Upregulation and Activation of the c-Jun/Fosl1 AP1 Complex Is Associated with EN-Mediated Transformation**

(A) AP1 EMSAs on nuclear lysates from control, EN, or EN kinase-dead (KD) transduced 3T3 cells. Incubation with a specific unlabeled competitor blocks band shift (lane 3). EN-3T3 nuclear lysates produced a significantly larger band shift compared to control or EN KD-3T3 lysates (compare lane 5 to lanes 2 and 6).

(B) Antibodies specific to Fosl1, Fosl2, and c-Jun band-shifted or destroyed the AP1 band shift produced by EN nuclear extracts, whereas antibodies to c-Fos and Sp1 had no effect.

(C) Western blot analysis performed on lysates from serum-starved control (MSCVp), kinase-dead EN (EN-KD), and EN 3T3 cells. EN cells possessed a tyrosine phosphorylated oncoprotein doublet and elevated levels of phosphorylated Akt, MEK, and c-Jun (ser 63 and 73) as well as elevated levels of Fosl1, total c-Jun, and cyclin D1/2. Loading control: Grb2.

(D) Immunofluorescence (Da–Dc and Dg–Di) and immunohistochemical (Dd–Df and Dj–Dl) staining of WT MGs (Da, Dd, Dg, and Dj), EN hyperplastic MGs (Db, De, Dh, and Dk), and EN mammary tumors (Dc, Df, Di, and Dl) with antibodies against Fosl1 (Da–Dc), phosphorylated c-Jun at Ser63 (Dd–Df) and at Ser73 (Dg–Di), and total c-Jun (Dj–Dl). WT MGs in (Da), (Dd), and (Dj) were from nulliparous female mice. WT MG in (Dg) was from a lactating female. Scale bars, 50 μm.

(E) Immunostaining of three SBC cases confirms the presence/activation of the c-JUN/FOSL1 AP1 complex. Scale bars, 50 μm.

*HBEGF* (heparin-binding EGF-like growth factor), *BCL2L11* (BIM), *CDKN1A* (p21), and *CDKN2A* (p16). $p16^{INK4A}$ and $p21^{WAF1}$ typically function as tumor suppressors. However, both may also act as oncogenes. In fact, overexpression of p16 is found in breast cancer cases with a more malignant phenotype (Milde-Langosch et al., 2001). Of note, we did not observe significant enrichment of this AP1 signature in sorted EN tumor cells compared to sorted EN hyperplastic MECs (Figure 5C and Figure S6C), suggesting that at least part of this signature might have already been acquired in hyperplastic MECs during the initial stage of EN transformation.

To confirm involvement of the c-Jun/Fosl1 AP1 complex in EN-mediated transformation, we performed electrophoretic mobility shift assays (EMSAs) on nuclear lysates from 3T3 cells and observed a significantly larger and specific band shift created by AP1 complex formation in EN-3T3 cells (Figure 6A). This AP1 complex was composed of

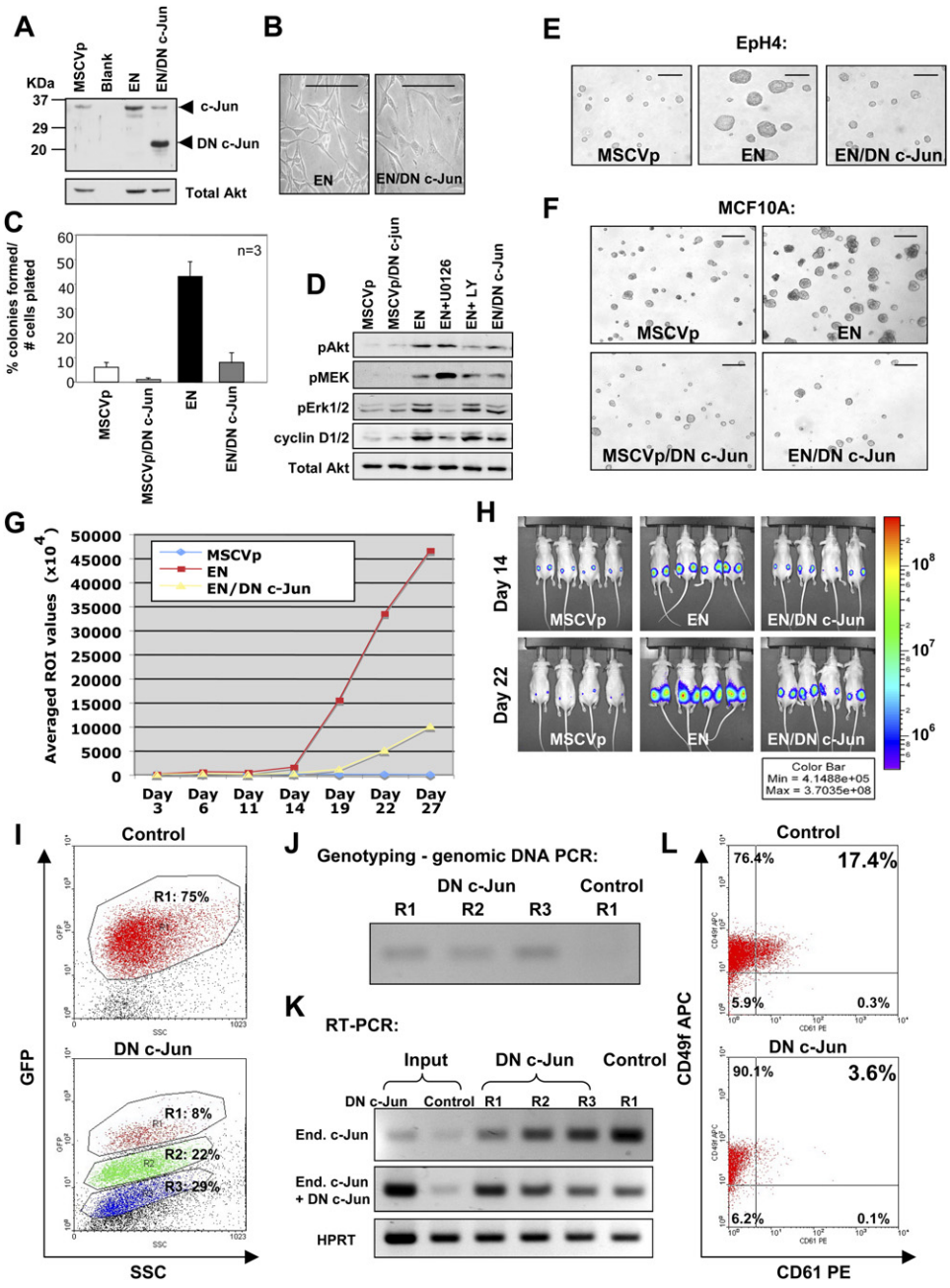


**Figure 7. Expression of a Dominant-Negative c-Jun Blocks EN-Mediated Transformation**

(A) Expression of dominant-negative (DN) c-Jun in EN-expressing cells confirmed by western blot analysis. Loading control: total Akt.

(B and C) DN c-Jun expression reverts EN-mediated morphological transformation ([B], scale bars, 50 μm) and soft agar colony formation ([C], error bars = mean ± SD) in 3T3 cells.

(D) Western blot analysis of serum-starved control cells (MSCVp) and EN cells (alone, coexpressing DN c-Jun, or treated with either MEK inhibitor U0126 or PI3K inhibitor LY294002 [LY] [25 μM]). Both U0126 treatment and coexpression of DN c-Jun had a significant effect upon cyclin D1/2 levels in EN cells. Loading control: total Akt.

(E) Effects of EN and DN c-Jun expression on EpH4 cell growth after 4 days in 3D Matrigel cultures. Scale bars, 500 μm.

(F) Effects of EN and DN c-Jun expression on human MCF10A cell growth in 3D Matrigel cultures. Scale bars, 1000 μm.

(G) Tumor growth curves of luciferase expressing cells injected subcutaneously into nude mice. ROI, regions of interest values in photons/s/cm$^2$/sr.

(H) Comparison of bioluminescent images of mice at day 14 and day 22.

(I) Top panel shows Gfp$^+$ cells in an empty-vector transduced EN tumor developed in the *Rag2*$^{-/-}$ host. Lower panel shows three distinct populations of Gfp$^+$ cells (R1–R3 express high, medium, and low levels of Gfp, respectively) in a DN c-Jun transduced EN tumor developed in the *Rag2*$^{-/-}$ host.

(J) PCR genotyping (using a forward primer in the DN c-Jun and a reverse primer in the PGK promoter of the viral vector) confirms integration of DN c-Jun viruses in all three populations (R1–R3) of the DN c-Jun/EN tumor. This primer set does not detect the control viruses (vector only).

c-Jun and Fosl1 or Fosl2 (Figure 6B). Western blot analysis confirmed significantly elevated levels of total c-Jun, phosphorylated c-Jun, and Fosl1 only in EN-3T3 cells (Figure 6C), suggesting that c-Jun/Fosl1 is indeed the major AP1 complex formed upon EN-mediated transformation.

To validate upregulation and activation of the c-Jun/Fosl1 complex in EN tumors, we performed immunostaining using antibodies against Fosl1, phosphorylated c-Jun, and total c-Jun. In WT MGs, Fosl1 is mainly localized in cytoplasm (Figure 6Da). In EN hyperplastic MECs and tumor cells, the overall intensity of Fosl1 staining is increased, and more importantly, significant Fosl1 nuclear staining is detected (Figures 6Db and 6Dc). In addition, upregulation and phosphorylation of c-Jun is also evident in EN hyperplastic MECs and tumor cells, but not in WT MGs (Figures 6Dd–6Dl), suggesting that activation of this AP1 complex is an early event (i.e., present in hyperplastic MECs) and persists in EN-mediated tumorigenesis.

To determine the c-Jun/Fosl1 status in human SBC, we stained three SBC cases with c-JUN and FOSL1 antibodies. As shown in Figure 6E, in three of three SBC samples studied, we detected nuclear staining of FOSL1, and expression and activation (phosphorylation) of c-JUN, suggesting that activation of the c-JUN/FOSL1 complex is indeed associated with human SBC.

## Expression of a Dominant-Negative c-Jun Blocks EN-Mediated Transformation

To determine if AP1 activation is necessary for EN-mediated transformation, we employed the dominant-negative (DN) c-Jun TAM67, which lacks its transactivation domain, to block the AP1 activity (Ludes-Meyers et al., 2001) in several different systems. Coexpression of DN c-Jun in EN-3T3 cells blocked EN-mediated transformation both morphologically and molecularly (Figures 7A–7D). Ectopic expression of EN in the murine EpH4 cells and human MCF10A cells led to larger spheroids in 3D Matrigel cultures, which was reverted by coexpression of DN c-Jun (Figures 7E and 7F). We have shown previously that EN-transduced EpH4 (EN-EpH4) cells formed tumors upon subcutaneous injection in immunodeficient mice (Tognon et al., 2002). We now show that expression of DN c-Jun in EN-EpH4 cells significantly reduces their tumorigenic properties in vivo (Figures 7G and 7H). We compared microarray expression profiles between EN-EpH4 tumors and DN c-Jun/EN-EpH4 tumors by GSEA. As expected, many gene sets enriched in sorted EN tumor cells (compared to unsorted EN tumors) are downregulated in DN c-Jun/EN-EpH4 tumors (Table S7). Importantly, one of them is "JNK_UP," a gene set directly related to JNK-JUN signaling.

Lastly, we asked whether forced expression of DN c-Jun in primary EN tumor cells impairs their capacity to form new tumors upon transplantation. We developed a protocol to retrovirally transduce EN tumor cells ex vivo quickly, sort virally infected $Gfp^+$ cells, and then transplant them into *Rag2*$^{-/-}$ mice immediately. In three independent experiments performed, five of five *Rag2*$^{-/-}$ mice transplanted with $Gfp^+$ EN tumor cells transduced by the control virus (empty vector, LPIG) developed tumors in 2∼3 months, whereas only three of five *Rag2*$^{-/-}$ mice transplanted with the same numbers of $Gfp^+$, DN c-Jun-transduced EN tumor cells developed tumors within the same time window. In one tumor derived from DN c-Jun-transduced EN tumor cells, we detected three distinct populations of tumor cells expressing high, medium, and low levels of Gfp (Figure 7I). Intriguingly, the $Gfp^{hi}$ population was significantly smaller than the other two. In contrast, the majority of tumor cells in the control (LPIG) tumor were $Gfp^+$ cells expressing high levels of Gfp. We individually sorted these distinct populations of $Gfp^+$ cells and confirmed they were all derived from virally transduced cells (Figure 7J). We then quantitated DN c-Jun expression levels and compared these to virally transduced cells before transplantation (i.e., input). Consistent with their Gfp expression levels, the $Gfp^{hi}$, $Gfp^{mid}$, and $Gfp^{low}$ cells in the DN c-Jun-transduced tumor also expressed high, medium, and low levels of DN c-Jun, respectively. In addition, even the $Gfp^{hi}$ tumor cells expressed much lower levels of DN c-Jun than those of the input (Figure 7K). These findings suggest that selection against EN tumor cells expressing high levels of DN c-Jun occurs in vivo. Upon staining with antibodies for stem/progenitor markers CD61 and CD49f, we found the DN c-Jun-transduced tumors contained fewer $CD61^+CD49f^+$ cells than the control tumors (Figure 7L). Since $CD61^+CD49f^+$ MECs may represent stem/progenitor cells in MGs (Asselin-Labat et al., 2007), we hypothesize that forced expression of DN c-Jun in EN tumor cells may reduce the number of tumor cells capable of initiating new tumors upon transplantation. Furthermore, in one *Rag2*$^{-/-}$ mouse transplanted with DN c-Jun-transduced EN tumor cells, two physically separated tumors developed. One tumor expressed high levels of Gfp and DN c-Jun; the other expressed lower levels of Gfp and DN c-Jun (data not shown). We sorted $Gfp^+$ cells from both tumors and serially transplanted the same numbers of sorted cells (ranging from 500 to $5 \times 10^5$) into *Rag2*$^{-/-}$ mice. 1.5 months after transplantation, *Rag2*$^{-/-}$ mice injected with $1 \times 10^5$ and $5 \times 10^5$ $Gfp^{low}$ (thus also DN c-$Jun^{low}$) cells have already developed new tumors, whereas none of the *Rag2*$^{-/-}$ mice transplanted with $Gfp^{hi}$ (thus also DN c-$Jun^{hi}$) cells have developed tumors. This again suggests that high levels of DN c-Jun expression in EN tumor cells reduce the number of tumor cells capable of forming new tumors upon transplantation.

(K) Expression levels of DN c-Jun are estimated indirectly by comparing expression levels of the endogenous c-Jun to those of total c-Jun (endogenous + DN c-Jun). Expression of the endogenous c-Jun is detected by a PCR primer set located in the region deleted in DN c-Jun. Expression of total c-Jun is detected by a second primer set located in the common region.
(L) Flow cytometry analysis shows reduced number of $CD61^+$ cells in the DN c-Jun/EN tumor compared to the control tumor. A representative experiment is shown.

## DISCUSSION

### Committed Mammary Progenitors as Cells of Origin for Breast Cancer

A central question in cancer biology is the cellular origin of cancers. Do cancers originate from normal stem cells that lose normal growth control, or do they initiate from progenitors or more differentiated cells after acquisition of stem cell attributes through mutation(s) (Lobo et al., 2007)? Current views are derived largely from studies of leukemias in the hematopoietic system. Since hematopoietic stem cells (HSCs) are endowed with self-renewal, it has been argued that transformation of HSCs provides a simple means to generate leukemic cells. Paradoxically, cellular phenotypes in diverse leukemias mirror those of progenitors, rather than HSCs (Lobo et al., 2007). In fact, evidence in both patients and mouse models favors a progenitor cell origin for many leukemias (e.g., see Jamieson et al., 2004; Krivtsov et al., 2006).

Similarly, although MaSCs are often proposed as cells of origin for breast tumors, cellular phenotypes of human breast cancer are not easily reconciled with this view. For instance, since MaSCs can give rise to both luminal and myoepithelial cells, one would expect to see mixed cell types in breast cancer if MaSCs represent the predominant cellular origin, yet most human breast tumors exhibit phenotypes of luminal epithelial cells (Sorlie et al., 2001). This suggests that more differentiated cells in MGs may serve as cells of origin for breast cancer. However, the existence of such committed progenitors in normal MGs remains to be directly demonstrated. Likewise, direct evidence is also lacking to show such cells as targets of transformation leading to breast cancer.

The cellular origin of human breast cancer is difficult to establish. Murine models, therefore, represent a tractable alternative for analysis. Previous studies using murine models have proposed both MaSCs and more differentiated cells, including mammary progenitors, as targets of breast cancer (Li and Rosen, 2005). Moreover, in murine models created by overexpression of oncogenes driven by the same promoter (e.g., *MMTV*), different oncogenes (e.g., Wnt1/β-catenin versus Neu or H-Ras or PyMT) appear to preferentially transform distinct populations of MECs. However, due to use of exogenous promoters (thus oncogenes often expressed at nonphysiological levels), and in the absence of genetic marking and thorough characterization of tumor cell types, these models cannot definitively assign target cells within the normal MEC developmental hierarchy.

In *WCEN* mice, *EN* is under the transcriptional control of the endogenous *Etv6* promoter and therefore should be expressed at a physiological level. Since mammary tumors develop in nulliparous *WCEN* females at 100% penetrance and transient *Wap*$^+$ cells are the only cells in which *EN* expression is activated, this unique combination and the genetic marking experiment described above provide direct evidence to support committed mammary progenitors (within the transient *Wap*$^+$ cells) as targets of EN.

Previous studies using genetic marking have identified a population of multipotent MECs (termed parity-induced MECs, or PI-MECs) that originate from *Wap-Cre*-expressing differentiating cells during the first pregnancy/lactating cycle, survive through postlactational remodeling, and persist throughout the remainder of life (Boulanger et al., 2005; Henry et al., 2004; Wagner et al., 2002; Wagner and Smith, 2005). Recently, a population of alveolar progenitor cells, similar to PI-MECs, was identified in nulliparous mouse MGs (Booth et al., 2007). These cells represent lobule-restricted multipotent progenitors capable of proliferation and differentiation to both luminal and myoepithelial cells upon transplantation. Apparently, these progenitor cells are targets of EN in *WCEN* virgin females, as described in this study.

Our study also supports the existence of an epithelial cell hierarchy in both normal MGs and in mammary tumors. We have described at least two types of committed alveolar progenitors in the transient population of *Wap*$^+$ MECs in nulliparous MGs: the bipotent alveolar progenitors as targets of type 1 tumors and the lineage-committed CD61$^+$ luminal alveolar progenitors as targets of type 2 tumors. However, we cannot exclude the possibility that type 2 tumors are also derived from bipotent progenitors that are blocked in differentiation and only give rise to CD61$^+$ immature luminal cells. We favor lineage-committed CD61$^+$ luminal progenitors, rather than bipotent progenitors, as their target cells. In support of this conclusion, knockout of *Gata3* in MGs led to an expansion of CD61$^+$ luminal progenitors and a concomitant block in differentiation (Asselin-Labat et al., 2007), suggesting the existence of such luminal-restricted progenitors in the normal MEC hierarchy. In some type 1 EN tumors, we observed regions with extensive K5$^+$K14$^+$p63$^+$ basal epithelial cells (type 1a), and regions with K8$^+$K14$^+$K5$^-$ immature luminal epithelial cells surrounded by K5$^+$K14$^+$p63$^+$ basal/myoepithelial cells (type 1b). This can be best explained by the existence of an epithelial cell hierarchy in EN tumors. The committed bipotent alveolar progenitors are transformed by EN and become oncogenic bipotent progenitors, which give rise to abnormal luminal-restricted progenitors and basal/myoepithelial-committed progenitors. In most cases, these progenitors differentiate into well-differentiated type 1 EN bipotent tumors. Occasionally, either under the influence of the microenvironment, or after acquiring additional mutations, some of the abnormal luminal or basal/myoepithelial-committed progenitors become further transformed and give rise to clones of immature luminal or basal epithelial cells (due to block in differentiation), respectively (Figure 8).

K14 is a type II keratin that pairs with the type I keratin K5 to form heterodimers in basal cells of stratified epithelia. Thus, both K5 and K14 have been considered as basal cell markers and have been used to distinguish basal/myoepithelial cells from K8$^+$ luminal epithelial cells. However, in this study, we show that K14 also stains a subset of K8$^+$ luminal epithelial cells, in addition to K5$^+$ basal/myoepithelial cells (Figure 4A and Figures S2A and S7). In fact, these K14$^+$K8$^+$ luminal cells represent blocked CD61$^+$

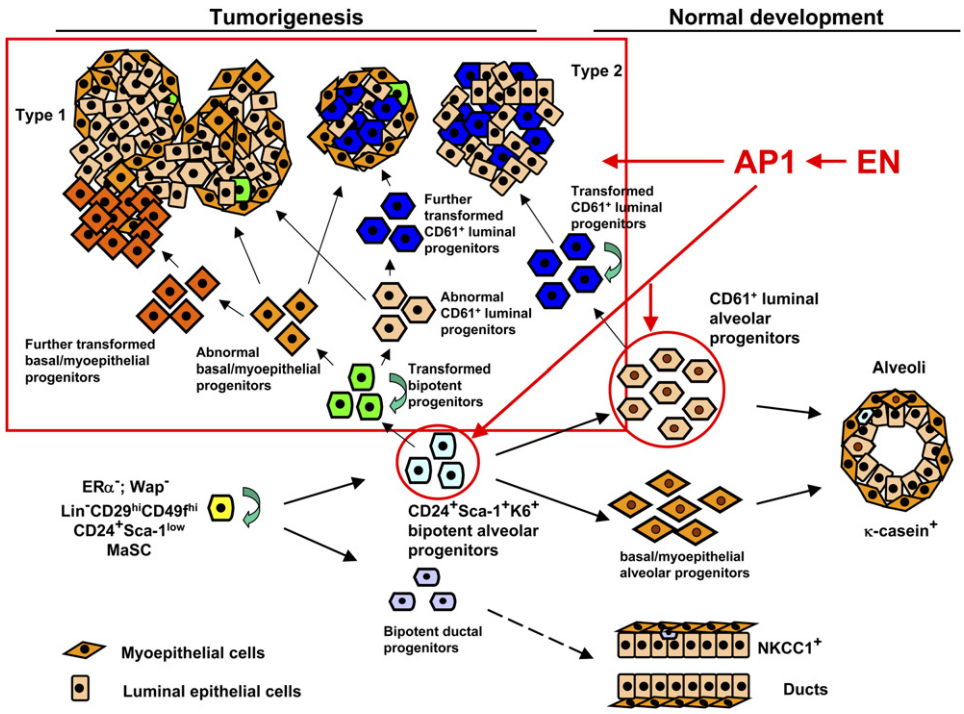


**Figure 8. The Mammary Epithelial Cell Hierarchy in Normal Mammary Glands and in Mammary Tumors from *Wap-Cre;EN* Females**
Proposed target cells of EN in *WCEN* females are indicated (red circles). Red arrows indicate that EN-initiated tumorigenesis (both tumor initiation and progression) is mediated through AP1.

luminal progenitors in EN tumors. Of note, in normal MGs, a population of $K14^+K8^+$ (Figure 4B, this study) or $K14^+K18^+$ luminal cells is also detected (Shackleton et al., 2006). In addition, our microarray analysis of murine breast cancer models also shows that the *K14* gene cluster is distinct from the *K5* basal gene cluster (Figure 4C; also Herschkowitz et al., 2007). Thus, K14 is distinct from K5 as a marker, and a combination of both markers together with other markers (e.g., p63, SMA, K8) can be used to define subpopulations of cells in murine mammary tumors.

Although we show that EN transforms committed alveolar progenitors, we do not dismiss the possibility that EN may also transform MaSCs. Interestingly, as we described above, due to the leaky expression of the *EN* allele (without Cre-mediated excision of the "stopper," thus independent of the *Wap* promoter), a small number of *EN*-only heterozygous mice develop mammary tumors at advanced ages. Most of these tumors fall within one of the four subtypes described above in *WCEN* females (Figure S7), suggesting that target cells of EN in these two types of mice are probably similar. However, under this genetic setting, one cannot be certain if bipotent tumors with type 1 features are derived from committed bipotent progenitors (similar to *WCEN*) or from MaSCs, since they probably give rise to tumors with a similar appearance. In addition to tumors with features of these four subtypes, we also observed tumors either containing extensively $K5^+$ basal cells, or containing mainly $K8^+$ (but $K14^-$) luminal cells (Figure S7). This is most likely due to the long latency of tumors that develop in *EN*-only mice (>1 year compared to several months for *WCEN* females). More differentiated, single lineage-committed cells may be transformed by EN after they accumulate additional mutations over an extended time period.

## Transformation by EN Oncoprotein Is Mediated through the AP1 Complex

The AP1 transcriptional complex is composed of heterodimeric Jun/Fos family proteins (Eferl and Wagner, 2003). The AP1 pathway integrates multiple growth signals at the transcriptional level and regulates several cellular processes (Shen et al., 2007). In normal MGs, previous studies have shown that AP1 is a pivotal regulator of postnatal MG growth and development (Shen et al., 2006). In human breast cancer, c-JUN activation is associated with proliferation and angiogenesis in invasive breast cancer (Vleugel et al., 2006). Overexpression of the DN c-Jun in breast cancer cells induces a G1 cell cycle block and inhibits their growth both in vitro and in vivo (Liu et al., 2002). Fosl1 (Fra1) regulates proliferation and invasiveness of breast cancer cells (Belguise et al., 2005; Milde-Langosch et al., 2004). Overexpression of FOSL1 (FRA-I) protein has been observed in both hyperplastic and neoplastic human breast disorders (Chiappetta et al., 2007). In addition, Fosl1 was also used as an effective target for a DNA vaccine to protect mice against breast cancer (Luo et al., 2003).

Our findings demonstrate that EN expression leads to upregulation and activation of the c-Jun/Fosl1 AP1 complex. Several AP1 target genes are upregulated in both EN-3T3 cells and EN tumor cells (Figures 5A and 5B and Figures S6A and S6B), including *HBEGF* and possibly *CCND1* (cyclin D1), which stimulate proliferation. Cyclin D1 is the major positive regulator of cell cycle progression induced by AP1 (Bakiri et al., 2000). Although we did not observe increased levels of cyclin D1 in sorted tumor cells directly compared to unsorted tumors (possibly due to its expression in stromal cells), we observed its upregulation in EN-3T3 cells both by microarray and western blot (Figures 2D and 5B). We demonstrated its upregulation during tumor progression (Figure 5C). We also detected high levels of cyclin D1/2 expression in EN tumors by western blot (Figure 2D). Intriguingly, our microarray analysis shows that several AP1 target genes known to promote angiogenesis and invasiveness, including *PLAUR*, *PLAU*, *CD44*, *CTSL* (cathepsin L), *MMP3* (matrix metallopeptidase 3), and *TPM3* (tropomyosin 3) are upregulated in both EN-3T3 cells and EN hyperplastic MECs (Figures 5B and 5C), suggesting that an EN/AP1-induced invasiveness program may be established early in EN-mediated transformation. This observation may partially account for the short latency and aggressiveness of EN tumors in mice, and the appearance of SBC in children as young as 3 years of age (Euhus et al., 2002).

Together with previous observations in human breast cancer cells, our study supports critical roles of AP1 in breast tumorigenesis and invasiveness. Further focus on this transcriptional complex as a target in human breast cancer is warranted.

## Modeling Chromosomal Rearrangements in Human Epithelial Tumors Can Provide Insights into Their Pathogenesis and Therapy

The breast cancer model described here is based on the t(12;15)(p13;q25) translocation in human cancer. Our data demonstrate that the translocation-generated EN fusion oncoprotein is sufficient to initiate mammary tumorigenesis. This complements genetic evidence in humans suggesting that this translocation is the primary event in the disorder (Tognon et al., 2002). In our model, *EN* is induced only in a very small number of cells in mammary tissues and the tumor cells emerge within the environment of normal cells, thus closely mimicking human disease initiated by somatic mutation. The recent findings of recurrent gene fusions in prostate cancer and lung cancer suggest that balanced, disease-specific chromosomal rearrangements in epithelial cancers may be more common and important than previously believed (Meyerson, 2007; Tomlins et al., 2005). As demonstrated in hematopoietic malignancies, study of gene rearrangements has contributed immeasurably to an understanding of both normal blood cell development and malignancy. In addition, study of gene fusions with kinase activities has revolutionized targeted therapies for cancer (e.g., imatinib for BCR-ABL fusion). We hope that the success in modeling an infrequent translocation seen in human epithelial cancer described here will inspire the generation of sophisticated models of other chromosomal arrangements that may occur more commonly in other epithelial tumors. Such engineered mice permit experimental access to the earliest target cells and steps in the transformation process and may serve as effective models for preclinical testing.

## EXPERIMENTAL PROCEDURES

### Mice

*Etv6-NTRK3* conditional knockin mice were generated by gene targeting (details are provided in the Supplemental Experimental Procedures). *Wap-Cre*, *MMTV-Cre*, and *Wap-rtTA-Cre* transgenic mice were acquired from the MMHCC repository at NCI-Frederick. *Rosa-Stop-lacZ* reporter mice and *Rag2*$^{-/-}$ immunodeficient mice are maintained in our mouse colony. The *Rosa-Stop-Luc* reporter was kindly provided by Dr. William G. Kaelin, Jr. All studies involving mice were approved by the Children's Hospital Boston Institutional Animal Care and Use Committee and performed in accordance with the relevant protocol.

### Human SBC Samples

The SBC cases were accrued from Pathology departments at Children's and Women's Health Centre of British Columbia, Instituto de Patologia e Imunologia Molecular da Universidade do Porto, and Burnaby General Hospital, Burnaby, Canada. Informed consent was obtained for all patient samples used in this study, and ethics approval was received from the Research Ethic Board (REB) at the University of British Columbia.

### Pathology, Immunostaining, *lac*Z Staining, and Flow Cytometry

Standard protocols were followed. Detailed procedures are provided in the Supplemental Experimental Procedures.

### Biochemical and Cellular Assays

Standard protocols were followed. Details about EMSAs, western blot, immunoprecipitation studies, and soft agar assays are provided in the Supplemental Experimental Procedures.

### Microarray Data Collection and Analysis

Microarray expression profiles were collected using Affymetrix or Agilent chips and analyzed using dChip (Li and Wong, 2001) and GSEA (Subramanian et al., 2005) as described. Details are provided in the Supplemental Experimental Procedures. All microarray data have been deposited in NCBI's Gene Expression Omnibus (GEO; http://www.ncbi.nlm.nih.gov/geo/) with GEO Series accession numbers GSE9355 (EN tumors using Affymetrix chips), GSE9354 (3T3 cells), GSE9353 (EpH4-derived tumors), and GSE9343 (selected EN tumors using Agilent chips).

### Supplemental Data

The Supplemental Data include Supplemental Experimental Procedures, seven supplemental figures, and eight supplemental tables and can be found with this article online at http://www.cancercell.org/cgi/content/full/12/6/542/DC1/.

## ACKNOWLEDGMENTS

We thank Dr. Yuko Fujiwara, Aimee Williams, and Nicole Stokes for help with transgenic mice; Carol Browne for assistance with ES cell targeting; Melanie Hamblen for general support; Grigoriy Losyev for cell sorting; Dr. Leonard Zon for discussion; Dr. Tim Triche for help with microarray of 3T3 cells. This work was supported by grants to S.H.O. from the NCI Mouse Models of Human Cancer Consortium and from the Department of Defense, by grants to P.H.S. from the Canadian Institutes for Health Research (CIHR), by funds to C.M.P. from

NCI (RO1-CA-101227-01) and HHSN-261200433008C (N01-CN43308), and by a K99 Pathway-to-Independence award to Z.L. from NCI. S.H.O. is an Investigator of the Howard Hughes Medical Institute. C.E.T. was supported by a ReThink Breast Cancer Career Development Award.

Received: December 20, 2006
Revised: August 29, 2007
Accepted: November 16, 2007
Published: December 10, 2007

## REFERENCES

Asselin-Labat, M.L., Sutherland, K.D., Barker, H., Thomas, R., Shackleton, M., Forrest, N.C., Hartley, L., Robb, L., Grosveld, F.G., van der Wees, J., et al. (2007). Gata-3 is an essential regulator of mammary-gland morphogenesis and luminal-cell differentiation. Nat. Cell Biol. *9*, 201–209.

Bakiri, L., Lallemand, D., Bossy-Wetzel, E., and Yaniv, M. (2000). Cell cycle-dependent variations in c-Jun and JunB phosphorylation: A role in the control of cyclin D1 expression. EMBO J. *19*, 2056–2068.

Belguise, K., Kersual, N., Galtier, F., and Chalbos, D. (2005). FRA-1 expression level regulates proliferation and invasiveness of breast cancer cells. Oncogene *24*, 1434–1444.

Booth, B.W., Boulanger, C.A., and Smith, G.H. (2007). Alveolar progenitor cells develop in mouse mammary glands independent of pregnancy and lactation. J. Cell. Physiol. *212*, 729–736.

Boulanger, C.A., Wagner, K.U., and Smith, G.H. (2005). Parity-induced mouse mammary epithelial cells are pluripotent, self-renewing and sensitive to TGF-beta1 expression. Oncogene *24*, 552–560.

Chiappetta, G., Ferraro, A., Botti, G., Monaco, M., Pasquinelli, R., Vuttariello, E., Arnaldi, L., Di Bonito, M., D'Aiuto, G., Pierantoni, G.M., and Fusco, A. (2007). FRA-1 protein overexpression is a feature of hyperplastic and neoplastic breast disorders. BMC Cancer *7*, 17.

Eferl, R., and Wagner, E.F. (2003). AP-1: A double-edged sword in tumorigenesis. Nat. Rev. Cancer *3*, 859–868.

Eguchi, M., Eguchi-Ishimae, M., Tojo, A., Morishita, K., Suzuki, K., Sato, Y., Kudoh, S., Tanaka, K., Setoyama, M., Nagamura, F., et al. (1999). Fusion of ETV6 to neurotrophin-3 receptor TRKC in acute myeloid leukemia with t(12;15)(p13;q25). Blood *93*, 1355–1363.

Euhus, D.M., Timmons, C.F., and Tomlinson, G.E. (2002). ETV6-NTRK3—Trk-ing the primary event in human secretory breast cancer. Cancer Cell *2*, 347–348.

Hennighausen, L., and Robinson, G.W. (2005). Information networks in the mammary gland. Nat. Rev. Mol. Cell Biol. *6*, 715–725.

Henry, M.D., Triplett, A.A., Oh, K.B., Smith, G.H., and Wagner, K.U. (2004). Parity-induced mammary epithelial cells facilitate tumorigenesis in MMTV-neu transgenic mice. Oncogene *23*, 6980–6985.

Herschkowitz, J.I., Simin, K., Weigman, V.J., Mikaelian, I., Usary, J., Hu, Z., Rasmussen, K.E., Jones, L.P., Assefnia, S., Chandrasekharan, S., et al. (2007). Identification of conserved gene expression features between murine mammary carcinoma models and human breast tumors. Genome Biol. *8*, R76.

Ince, T.A., Richardson, A.L., Bell, G.W., Saitoh, M., Godar, S., Karnoub, A.E., Iglehart, J.D., and Weinberg, R.A. (2007). Transformation of different human breast epithelial cell types leads to distinct tumor phenotypes. Cancer Cell *12*, 160–170.

Jamieson, C.H., Ailles, L.E., Dylla, S.J., Muijtjens, M., Jones, C., Zehnder, J.L., Gotlib, J., Li, K., Manz, M.G., Keating, A., et al. (2004). Granulocyte-macrophage progenitors as candidate leukemic stem cells in blast-crisis CML. N. Engl. J. Med. *351*, 657–667.

Knezevich, S.R., Garnett, M.J., Pysher, T.J., Beckwith, J.B., Grundy, P.E., and Sorensen, P.H. (1998a). ETV6-NTRK3 gene fusions and trisomy 11 establish a histogenetic link between mesoblastic nephroma and congenital fibrosarcoma. Cancer Res. *58*, 5046–5048.

Knezevich, S.R., McFadden, D.E., Tao, W., Lim, J.F., and Sorensen, P.H. (1998b). A novel ETV6-NTRK3 gene fusion in congenital fibrosarcoma. Nat. Genet. *18*, 184–187.

Kordon, E.C., McKnight, R.A., Jhappan, C., Hennighausen, L., Merlino, G., and Smith, G.H. (1995). Ectopic TGF beta 1 expression in the secretory mammary epithelium induces early senescence of the epithelial stem cell population. Dev. Biol. *168*, 47–61.

Krivtsov, A.V., Twomey, D., Feng, Z., Stubbs, M.C., Wang, Y., Faber, J., Levine, J.E., Wang, J., Hahn, W.C., Gilliland, D.G., et al. (2006). Transformation from committed progenitor to leukaemia stem cell initiated by MLL-AF9. Nature *442*, 818–822.

Lamb, R.F., Hennigan, R.F., Turnbull, K., Katsanakis, K.D., MacKenzie, E.D., Birnie, G.D., and Ozanne, B.W. (1997). AP-1-mediated invasion requires increased expression of the hyaluronan receptor CD44. Mol. Cell. Biol. *17*, 963–976.

Li, Y., and Rosen, J.M. (2005). Stem/progenitor cells in mouse mammary gland development and breast cancer. J. Mammary Gland Biol. Neoplasia *10*, 17–24.

Li, C., and Wong, W.H. (2001). Model-based analysis of oligonucleotide arrays: Expression index computation and outlier detection. Proc. Natl. Acad. Sci. USA *98*, 31–36.

Liu, Y., Ludes-Meyers, J., Zhang, Y., Munoz-Medellin, D., Kim, H.T., Lu, C., Ge, G., Schiff, R., Hilsenbeck, S.G., Osborne, C.K., and Brown, P.H. (2002). Inhibition of AP-1 transcription factor causes blockade of multiple signal transduction pathways and inhibits breast cancer growth. Oncogene *21*, 7680–7689.

Lobo, N.A., Shimono, Y., Qian, D., and Clarke, M.F. (2007). The biology of cancer stem cells. Annu. Rev. Cell Dev. Biol. *23*, 675–699.

Ludes-Meyers, J.H., Liu, Y., Munoz-Medellin, D., Hilsenbeck, S.G., and Brown, P.H. (2001). AP-1 blockade inhibits the growth of normal and malignant breast cells. Oncogene *20*, 2771–2780.

Luo, Y., Zhou, H., Mizutani, M., Mizutani, N., Reisfeld, R.A., and Xiang, R. (2003). Transcription factor Fos-related antigen 1 is an effective target for a breast cancer vaccine. Proc. Natl. Acad. Sci. USA *100*, 8850–8855.

Mann, B., Gelos, M., Siedow, A., Hanski, M.L., Gratchev, A., Ilyas, M., Bodmer, W.F., Moyer, M.P., Riecken, E.O., Buhr, H.J., and Hanski, C. (1999). Target genes of beta-catenin-T cell-factor/lymphoid-enhancer-factor signaling in human colorectal carcinomas. Proc. Natl. Acad. Sci. USA *96*, 1603–1608.

Mao, X., Fujiwara, Y., and Orkin, S.H. (1999). Improved reporter strain for monitoring Cre recombinase-mediated DNA excisions in mice. Proc. Natl. Acad. Sci. USA *96*, 5037–5042.

Meyerson, M. (2007). Cancer: Broken genes in solid tumours. Nature *448*, 545–546.

Milde-Langosch, K., Bamberger, A.M., Rieck, G., Kelp, B., and Loning, T. (2001). Overexpression of the p16 cell cycle inhibitor in breast cancer is associated with a more malignant phenotype. Breast Cancer Res. Treat. *67*, 61–70.

Milde-Langosch, K., Roder, H., Andritzky, B., Aslan, B., Hemminger, G., Brinkmann, A., Bamberger, C.M., Loning, T., and Bamberger, A.M. (2004). The role of the AP-1 transcription factors c-Fos, FosB, Fra-1 and Fra-2 in the invasion process of mammary carcinomas. Breast Cancer Res. Treat. *86*, 139–152.

Reya, T., Morrison, S.J., Clarke, M.F., and Weissman, I.L. (2001). Stem cells, cancer, and cancer stem cells. Nature *414*, 105–111.

Robinson, G.W., McKnight, R.A., Smith, G.H., and Hennighausen, L. (1995). Mammary epithelial cells undergo secretory differentiation in cycling virgins but require pregnancy for the establishment of terminal differentiation. Development *121*, 2079–2090.

Robinson, G.W., Smith, G.H., Gallahan, D., Zimmer, A., Furth, P.A., and Hennighausen, L. (1996). Understanding mammary gland development through the imbalanced expression of growth regulators. Dev. Dyn. *206*, 159–168.

Rowley, J.D. (2001). Chromosome translocations: Dangerous liaisons revisited. Nat. Rev. Cancer *1*, 245–250.

Rubin, B.P., Chen, C.J., Morgan, T.W., Xiao, S., Grier, H.E., Kozakewich, H.P., Perez-Atayde, A.R., and Fletcher, J.A. (1998). Congenital mesoblastic nephroma t(12;15) is associated with ETV6-NTRK3 gene fusion: Cytogenetic and molecular relationship to congenital (infantile) fibrosarcoma. Am. J. Pathol. *153*, 1451–1458.

Safran, M., Kim, W.Y., Kung, A.L., Horner, J.W., DePinho, R.A., and Kaelin, W.G., Jr. (2003). Mouse reporter strain for noninvasive bioluminescent imaging of cells that have undergone Cre-mediated recombination. Mol. Imaging *2*, 297–302.

Shackleton, M., Vaillant, F., Simpson, K.J., Stingl, J., Smyth, G.K., Asselin-Labat, M.L., Wu, L., Lindeman, G.J., and Visvader, J.E. (2006). Generation of a functional mammary gland from a single stem cell. Nature *439*, 84–88.

Shen, Q., Zhang, Y., Uray, I.P., Hill, J.L., Kim, H.T., Lu, C., Young, M.R., Gunther, E.J., Hilsenbeck, S.G., Chodosh, L.A., et al. (2006). The AP-1 transcription factor regulates postnatal mammary gland development. Dev. Biol. *295*, 589–603.

Shen, Q., Uray, I.P., Li, Y., Krisko, T.I., Strecker, T.E., Kim, H.T., and Brown, P.H. (2007). The AP-1 transcription factor regulates breast cancer cell growth via cyclins and E2F factors. Oncogene. Published online July 16, 2007. 10.1038/sj.onc.1210643.

Simpson, P.T., Reis-Filho, J.S., Gale, T., and Lakhani, S.R. (2005). Molecular evolution of breast cancer. J. Pathol. *205*, 248–254.

Soda, M., Choi, Y.L., Enomoto, M., Takada, S., Yamashita, Y., Ishikawa, S., Fujiwara, S.I., Watanabe, H., Kurashina, K., Hatanaka, H., et al. (2007). Identification of the transforming EML4-ALK fusion gene in non-small-cell lung cancer. Nature *448*, 561–566.

Sorlie, T., Perou, C.M., Tibshirani, R., Aas, T., Geisler, S., Johnsen, H., Hastie, T., Eisen, M.B., van de Rijn, M., Jeffrey, S.S., et al. (2001). Gene expression patterns of breast carcinomas distinguish tumor subclasses with clinical implications. Proc. Natl. Acad. Sci. USA *98*, 10869–10874.

Stingl, J., Eirew, P., Ricketson, I., Shackleton, M., Vaillant, F., Choi, D., Li, H.I., and Eaves, C.J. (2006). Purification and unique properties of mammary epithelial stem cells. Nature *439*, 993–997.

Subramanian, A., Tamayo, P., Mootha, V.K., Mukherjee, S., Ebert, B.L., Gillette, M.A., Paulovich, A., Pomeroy, S.L., Golub, T.R., Lander, E.S., and Mesirov, J.P. (2005). Gene set enrichment analysis: A knowledge-based approach for interpreting genome-wide expression profiles. Proc. Natl. Acad. Sci. USA *102*, 15545–15550.

Tognon, C., Garnett, M., Kenward, E., Kay, R., Morrison, K., and Sorensen, P.H. (2001). The chimeric protein tyrosine kinase ETV6-NTRK3 requires both Ras-Erk1/2 and PI3-kinase-Akt signaling for fibroblast transformation. Cancer Res. *61*, 8909–8916.

Tognon, C., Knezevich, S.R., Huntsman, D., Roskelley, C.D., Melnyk, N., Mathers, J.A., Becker, L., Carneiro, F., MacPherson, N., Horsman, D., et al. (2002). Expression of the ETV6-NTRK3 gene fusion as a primary event in human secretory breast carcinoma. Cancer Cell *2*, 367–376.

Tomlins, S.A., Rhodes, D.R., Perner, S., Dhanasekaran, S.M., Mehra, R., Sun, X.W., Varambally, S., Cao, X., Tchinda, J., Kuefer, R., et al. (2005). Recurrent fusion of TMPRSS2 and ETS transcription factor genes in prostate cancer. Science *310*, 644–648.

Tomlins, S.A., Mehra, R., Rhodes, D.R., Smith, L.R., Roulston, D., Helgeson, B.E., Cao, X., Wei, J.T., Rubin, M.A., Shah, R.B., and Chinnaiyan, A.M. (2006). TMPRSS2:ETV4 gene fusions define a third molecular subtype of prostate cancer. Cancer Res. *66*, 3396–3400.

Tomlins, S.A., Laxman, B., Dhanasekaran, S.M., Helgeson, B.E., Cao, X., Morris, D.S., Menon, A., Jing, X., Cao, Q., Han, B., et al. (2007). Distinct classes of chromosomal rearrangements create oncogenic ETS gene fusions in prostate cancer. Nature *448*, 595–599.

Utomo, A.R., Nikitin, A.Y., and Lee, W.H. (1999). Temporal, spatial, and cell type-specific control of Cre-mediated DNA recombination in transgenic mice. Nat. Biotechnol. *17*, 1091–1096.

Vleugel, M.M., Greijer, A.E., Bos, R., van der Wall, E., and van Diest, P.J. (2006). c-Jun activation is associated with proliferation and angiogenesis in invasive breast cancer. Hum. Pathol. *37*, 668–674.

Wagner, K.U., Wall, R.J., St-Onge, L., Gruss, P., Wynshaw-Boris, A., Garrett, L., Li, M., Furth, P.A., and Hennighausen, L. (1997). Cre-mediated gene deletion in the mammary gland. Nucleic Acids Res. *25*, 4323–4330.

Wagner, K.U., Boulanger, C.A., Henry, M.D., Sgagias, M., Hennighausen, L., and Smith, G.H. (2002). An adjunct mammary epithelial cell population in parous females: Its role in functional adaptation and tissue renewal. Development *129*, 1377–1386.

Wagner, K.U., and Smith, G.H. (2005). Pregnancy and stem cell behavior. J. Mammary Gland Biol. Neoplasia *10*, 25–36.

Wai, D.H., Knezevich, S.R., Lucas, T., Jansen, B., Kay, R.J., and Sorensen, P.H. (2000). The ETV6-NTRK3 gene fusion encodes a chimeric protein tyrosine kinase that transforms NIH3T3 cells. Oncogene *19*, 906–915.

Welm, B.E., Tepera, S.B., Venezia, T., Graubert, T.A., Rosen, J.M., and Goodell, M.A. (2002). Sca-1(pos) cells in the mouse mammary gland represent an enriched progenitor cell population. Dev. Biol. *245*, 42–56.

## Accession Numbers

All microarray data have been deposited in NCBI's Gene Expression Omnibus (GEO; http://www.ncbi.nlm.nih.gov/geo/) with GEO Series accession numbers GSE9355 (EN tumors using Affymetrix chips), GSE9354 (3T3 cells), GSE9353 (EpH4-derived tumors), and GSE9343 (selected EN tumors using Agilent chips).